Journal Pre-proofs

Research paper

Ocular permeability, intraocular biodistribution of lipid nanocapsule formulation intended for retinal drug delivery

Gustav Christensen, Dileep Urimi, Laura Lorenzo-Soler, Nicolaas Schipper, François Paquet-Durand

PII: S0939-6411(23)00092-9
DOI: https://doi.org/10.1016/j.ejpb.2023.04.012
Reference: EJPB 14000

To appear in: *European Journal of Pharmaceutics and Biopharmaceutics*

Received Date: 31 January 2023
Revised Date: 5 April 2023
Accepted Date: 17 April 2023

Please cite this article as: G. Christensen, D. Urimi, L. Lorenzo-Soler, N. Schipper, F. Paquet-Durand, Ocular permeability, intraocular biodistribution of lipid nanocapsule formulation intended for retinal drug delivery, *European Journal of Pharmaceutics and Biopharmaceutics* (2023), doi: https://doi.org/10.1016/j.ejpb.2023.04.012

This is a PDF file of an article that has undergone enhancements after acceptance, such as the addition of a cover page and metadata, and formatting for readability, but it is not yet the definitive version of record. This version will undergo additional copyediting, typesetting and review before it is published in its final form, but we are providing this version to give early visibility of the article. Please note that, during the production process, errors may be discovered which could affect the content, and all legal disclaimers that apply to the journal pertain.

© 2023 The Author(s). Published by Elsevier B.V.

Ocular permeability, intraocular biodistribution of lipid nanocapsule formulation intended for retinal drug delivery

Gustav Christensen[a,1], Dileep Urimi[b,c,1], Laura Lorenzo-Soler[c], Nicolaas Schipper[b,*], François Paquet-Durand[a,*]

[a]Institute for Ophthalmic Research, University of Tübingen, Elfriede-Aulhorn Straße 5-7, 72076 Tübingen, Germany.
[b]Division Bioeconomy and Health, Chemical Process and Pharmaceutical Development, RISE Research Institutes of Sweden, Forskargatan 18, Södertälje 151 36, Sweden.
[c]Faculty of Pharmaceutical Sciences, School of Health Sciences, University of Iceland, Hofsvallagata 53, Reykjavík IS-107, Iceland.

* Corresponding authors

Nicolaas Schipper: nicolaas.schipper@ri.se
François Paquet-Durand: francois.paquet-durand@uni-tuebingen.de

[1] Gustav Christensen and Dileep Urimi contributed equally to this work.

Conflicts of Interest: The authors declare no conflicts of interest.

Journal Pre-proofs

Abstract

Recently, cGMP analogues have been investigated for the treatment of inherited retinal degenerations (IRD) using intravitreal injections. However, higher vitreous elimination rates limit the possibility to treat the retina with small molecule drugs. Here, we investigated the potential of lipid nanocapsules (LNCs) as vehicles to reduce clearance and prolong the delivery of cGMP analogue, CN03 to the retinal photoreceptors. Initially LNCs were investigated for both topical/periocular and intravitreal administration routes. While LNC-mediated drug permeation through the cornea proved to be too low for clinical applications, intravitreal application showed significant promise. Intravitreally administered LNCs containing fluorescent tracer in *ex vivo* porcine eyes showed complete intravitreal dispersal within 24 h. Ocular bio-distribution on histological sections showed that around 10 % of the LNCs had reached the retina, and 40 % accumulated in the ciliary body. For comparison, we used fluorescently labeled liposomes and these showed a different intraocular distribution with 48 % accumulated in the retina, and almost none were in the ciliary body. LNCs were then tested in retinal explants prepared from wild-type (WT) and *rd1* mouse. In WT retina LNCs showed no significant toxic effects up to a concentration of 5 mg/mL. In *rd1* retina, the LNC/CN03 formulation protected *rd1* photoreceptors with similar efficacy to that of free CN03, demonstrating the usefulness of LNC/CN03 formulation in the treatment of IRD. Overall, our results indicate the suitability of LNCs for intraocular administration and drug delivery to both the retina and the ciliary body.

Key words

Inherited retinal degenerations; Lipid nanocapsules; Liposomes; Intravitreal injections; Explant cultures; Drug delivery

Abbreviations

IRD, inherited retinal degenerations; LNCs, lipid nanocapsules; cGMP, cyclic guanosine- 3′,5′-monophosphate; IVT, intravitreal administration; TUNEL, terminal deoxynucleotidyl transferase dUTP nick end labeling; ONL, outer nuclear layer; INL, inner nuclear layer

Journal Pre-proofs

1. Introduction

Inherited retinal degeneration (IRD) relates to a group of rare diseases that result in the progressive loss of retinal photoreceptors, eventually leading to blindness [1-3]. Most of these diseases are untreatable to date and therapy development is hindered by, among other things, the vast genetic diversity of IRD combined with the various ocular barriers which limit drug access to photoreceptors [4].

In many IRD diseases, including in retinitis pigmentosa and Leber´s congenital amaurosis, pathological levels of intracellular cGMP have been identified [5]. Based on this mechanistic insight, cGMP analogues have been prepared to inhibit cGMP-activated targets within photoreceptors. One such analogue, CN03, was previously shown to produce morphological preservation of rod photoreceptors, as well as functional protection of cone photoreceptors in IRD mouse models, when administered in a liposomal drug delivery system [6]. The structure of CN03 is given in Fig. 1.

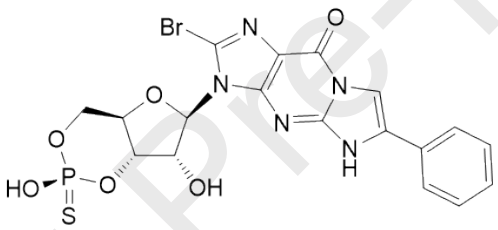

Fig. 1. Molecular structure of CN03

Recently, lipid-nanocapsules (LNC) have been investigated for CN03 encapsulation and release [7, 8]. It was found that LNCs achieved high drug encapsulation efficiency and sustained the release *in vitro* for up to 6 days, noticeably superior to what might be expected for the liposomal release of small hydrophilic compounds [9, 10]. LNCs are widely investigated for the treatment of various disease conditions mainly due to their biocompatibility, adaptability to modifications, and ease of preparation. LNCs are a type of core-shell nanoparticles that offer the possibility of loading various types of drug molecules including both hydrophilic and hydrophobic compounds of different molecular sizes. Unfortunately, LNC suitability for ocular administration is not very well understood and only a few reports are available, most of which focus on topical applications [11-13]. Due to ocular barrier restrictions, topical administration usually involves very little or no drug delivery to the retinal cells [14]. Intravitreal (IVT) administration is much more efficient for the treatment of retinal diseases as the injected solution is brought into close proximity to the target tissue [15, 16].

Here, we studied the permeation of LNCs using excised ocular tissues, and the bio-distribution of LNCs after an IVT injection in whole *ex vivo* porcine eyeballs, which have previously been used as a model for studying IVT particle distribution [17, 18]. IVT bio-distribution data was compared against that of liposomes. Moreover, the cytotoxicity of empty particles and the efficacy of CN03 loaded LNCs against photoreceptor cell death were assessed using organotypic retinal explant cultures derived from mice.

Journal Pre-proofs

2. Materials

1-palmitoyl-2-oleoyl-sn-glycero-3-phosphocholine (POPC), cholesterol, 1,2-distearoyl-sn-glycero-3-phosphoethanolamine-N-[methoxy(polyethylene glycol)-2000] (ammonium salt) (DSPE-PEG_{2000}), 3,3′-Dioctadecyl-oxacarbocyanin-perchlorate, dioctadecyl-3,3,3,3 Tetramethylindodicarbocyanine (DiO), Float-A-Lyzer® G2 dialysis devices (MWCO 100 kDa), chloroform, PBS, 4 % paraformaldehyde in PBS (PFA), sucrose and sodium chloride were obtained from Sigma Aldrich. Labrafac™ lipophile WL 1349 (Medium chain triglycerides, Ph. Eur. Grade), Kolliphor® HS 15 (polyethylene glycol (15)-hydroxystearate, Ph. Eur. Grade), and Phospholipon® 90 H (hydrogenated phosphatidylcholine ≥ 90 %) were obtained from Gattefossé (France), BASF and, Lipoid (Germany) respectively. The CN03 (also referred to as DF003 in previous publications) drug compound (R_P-8-Br-PET-cGMPS) was synthesized internally by RISE Research Institutes of Sweden [19].

3. Methods

3.1. Preparation of lipid nanocapsules

LNCs were prepared using a phase inversion process [7, 8]. In brief, the components of LNCs (Labrafac lipophile WL 1349, Kolliphor HS 15, Phospholipon 90 H, sodium chloride) along with DiO or CN03 were weighed and subjected to 3 heat-cool cycles of 90° C-60 °C. During the last cooling cycle, near the phase inversion temperature, an excess of cold water was added to the mixture to form the LNCs loaded with either DiO or CN03. For DiO the encapsulation efficiency was estimated to be around 100 % (from visual inspection of the aqueous phase). For comparison, blank LNC formulation was prepared in a similar way. Finally, LNCs were filtered using a 0.22 µM syringe filter and stored at 2-8 °C until further use.

3.2. Preparation of liposomes

Liposomes were prepared using an established protocol [20]. The compounds POPC, cholesterol, DSPE-PEG_{2000}, and DiO were dissolved in chloroform and mixed in the molar ratio 63.3:31.7:5:0.2. The chloroform was removed on a rotary evaporator (model RC600, KNF Neuberger, Trenton, NJ, USA) at 100 rpm and a pressure of 300 mbar for 1 to 2 h. The dried lipid film was hydrated in PBS and extruded using a mini-extruder (Avanti Polar Lipids, Alabaster, AL, USA) by passing the solution back and forth between a 100 nm porous polycarbonate membrane eleven times with Hamilton syringes. The liposomes were kept in the dark and stored at 2-8 °C until further use.

Journal Pre-proofs

3.3. Characterization of lipid nanocapsules

3.3.1. Physico-chemical characterization

3.3.1.1. Particle size and zeta potential measurements

Particle size, size distribution and zeta potential of the prepared LNCs were measured with a Malvern Zetasizer ZS (Malvern Instruments, UK). Size measurements were performed by dynamic light scattering (DLS) with an angle of detection of 173°. The zetapotential of LNCs was calculated by determining the electrophoretic mobility. Both size and zeta potential measurements were performed at 25 °C.

3.3.1.2. Release of DiO from LNCs

Release experiments on DiO loaded LNCs were performed in phosphate buffer using a dialysis setup. 1 mL of DiO-LNCs were placed in a Float-A-lyzer device with a 50kD MWCO membrane and this was kept in 18mL of phosphate buffer. Prior to the experiments, the dialysis device was pretreated as per the suppliers' standard instructions. Experiments were performed at 37 °C and stirring was maintained in the release buffer. At predetermined time intervals samples were collected for analysis and the whole buffer was replaced with fresh phosphate buffer. DiO released into the phosphate buffer was quantified by measuring the fluorescence intensity using a Varioskan™ LUX multimode microplate reader (ThermoFisher Scientific).

3.3.2. *Ex vivo* and *in vitro* characterization

3.3.2.1. Permeation of free drug and drug loaded LNCs in Franz-type diffusion cells

Fresh porcine eyes were obtained from a local slaughterhouse and were frozen at -80 °C within 2 h of collection until they were being used [21]. Before the tissue collection, the frozen eyes were brought to complete thaw by keeping them in PBS. After thawing, a small cut was made with the scalpel at the limbus and the corneas were dissected from the eyeballs. Full-thickness corneas and the conjunctiva-sclera-choroid-retina complex were isolated, and the permeability studies were performed using Franz-diffusion cells (PermeGear Inc., Pennsylvania, USA) using a similar process described by Pescina *et al*. [22, 23] with some modifications. The dissected tissues were kept between the donor and the receptor compartment with the endothelial side facing the receiving compartment. The donor compartment was filled with 1 mL of either free drug or drug loaded LNCs (LNC/CN03) at a concentration of 2 mg/mL, and phosphate buffer (5 mL) was used in the receptor compartment. Experiments were performed for up to 6 h at 37 ± 0.2 °C with constant stirring in the receptor buffer to avoid any boundary

Journal Pre-proofs

layer effect. At predetermined time intervals, 0.2 mL of sample was collected from the receptor compartment and was replaced with an equal volume of fresh buffer. Drug concentrations were measured using a microplate reader equipped with a UV–Vis spectrophotometric detector (SpectraMax, Molecular Devices, San Jose, CA) and the permeability coefficients were calculated using the algorithm described by Niedorf *et al.* [24]. All experiments were carried out in triplicate using different ocular bulbs from different animals.

3.3.2.2. Intraocular bio-distribution in *ex vivo* porcine eyes

Porcine eyes were obtained from a local slaughterhouse in the morning of the day of slaughter. The eyes were washed briefly in 70 % ethanol and sterile PBS. Excess tissue was removed. Before injection, the green background fluorescence along the axial length within the eyes were measured on an ocular fluorometer (FM-2 Fluorotron Master, OcuMetrics, CA, USA). A 50 µL volume of LNC/DiO or liposomes/DiO was injected into the center of the vitreous using a 22-gauge needle (Hamilton 1705 RN syringe, Hamilton, Reno, NV, USA). For LNC/DiO injected eyes, the green fluorescence signal from DiO was measured on the fluorometer directly after injection (t = 0), followed by incubation on a rotation shaker at 45 rpm. Additional measurements were recorded after 0.5 h, 1 h, 2 h, 6 h, and 24 h to follow the distribution of the particles. After the 24 h time-point, the eyes were fixed in a 4 % PFA solution following an established protocol [17]. After 5 days incubation at 2-8 °C, the eyes were washed twice in PBS and submerged in embedding medium (Tissue-Tek O.C.T. Compound, Sakura Finetek Europe, Alphen aan den Rijn, Netherlands) and frozen with liquid N_2. The eyes were sectioned on a cryostat (NX50, Thermo Fisher, Waltham, MA, USA) at –16 °C in 40 µm thick sections, which were transferred onto glass slides (Superfrost Plus™, R. Langenbrinck, Emmendingen, Germany). The slides were dried at 37 °C for 1-2 h in the dark, rehydrated with PBS for 10 min and mounted with Vectashield medium containing DAPI (Vector laboratories, Burlingame, CA, USA). They were kept at 2-8 °C for at least 0.5 h before imaging with fluorescent microscopy. The green signal was measured from different regions in the eye sections: the cornea, the lens, the ciliary body, the vitreous, and the retina. Sections from eyes where no particles were injected were used to qualitatively determine the baseline for a positive signal. For either LNC/DiO or liposome/DiO injected eyes, sections from 5 different eyes were measured (n = 5). One-way ANOVA with Tukey's multiple comparison test was calculated with GraphPad Prism 8 (GraphPad Software, San Diego, CA, USA) to determine statistical significances.

3.3.2.3. Retinal toxicity profile

Mice were sacrificed at post-natal day (P) 9 by cervical dislocation. The eyes were collected, and organotypic retinal explant cultures were prepared using an established protocol [25]. At P11, a 20 µL drop of either 0, 1, 5, or 10 mg/mL LNCs was added onto the side of the retina that would normally be in contact with the vitreous, *i.e.,* on top of retinal explant cultures. At P13, another drop of LNC solution was applied. At P15, the retinal explant cultures were fixed in PFA for 45 min, washed twice in PBS, and cryoprotected in 10 %, 20 %, and 30 % sucrose for 10 min, 20 min, and 30 min, consecutively. The retinal cultures were placed in embedding medium (Tissue-Tek O.C.T. Compound, Sakura Finetek Europe, Alphen aan den Rijn, Netherlands), snap-frozen in liquid N_2, and sectioned on a cryostat (NX50, Thermo Fisher, Waltham, MA, USA) at –20 °C into 14 µm sections, which were collected onto glass slides (Superfrost Plus™, R. Langenbrinck, Emmendingen, Germany). The slides were dried at 37 °C for 45 min and stored at –20 °C. To determine the amount of dying cells in the retinal tissue sections, a terminal deoxynucleotidyl transferase dUTP nick end labeling (TUNEL) assay was employed (TMR red, Product No. 12156792910, Sigma Aldrich, Darmstadt, Germany). The procedure is described under [26]. Afterwards, the slides were mounted with Vectashield containing DAPI and imaged using fluorescence microscopy. From the imaged sections, the relative amount of dying cells (TUNEL+ cells) were calculated from the following equation:

$$\text{TUNEL + cells (\%)} = \frac{N_{TUNEL}}{A_L/A_n} \cdot 100$$

Where N_{TUNEL} is the absolute number of TUNEL+ cells in either the outer nuclear layer (ONL) or the inner nuclear layer (INL) of the retinal tissue sections, A_L is the area of each layer, and A_n is the average area of the cells in each layer. For each condition, the relative TUNEL+ cells were determined for 4-5 different cultures (n = 4-5). Statistical analysis: One-way ANOVA with Tukey's multiple comparison test using GraphPad Prism 8.

3.3.2.4. Treatment efficacy of encapsulated CN03

The retinal degeneration *rd1* mouse model was used to produce organotypic retinal explant cultures at P5. At P7, LNC/CN03 formulation was applied to the culture in a drop onto the ganglion cell side of the cultures. Alternatively, a solution of free CN03 in 25 mM HEPES and 125 mM NaCl (pH 7.4) was applied. In both instances, the initial drug concentration in the solution applied to the retinal cultures was 200 µM, which, if assuming an even distribution across the culture medium, produced a final concentration of 4 µM. Non-treated cultures were

used as controls. LNC/CN03 administration was repeated at P9. At P11, the cultures were fixed, cryoprotected, frozen, and sectioned as described above. Additionally, organotypic retinal explant cultures from wild-type mice were prepared and left non-treated following the same paradigm. To determine the effect of CN03, cell death was determined using the TUNEL assay as described above. From the imaged sections, the relative amount of dying cells (TUNEL+ cells) were calculated from the equation above. The relative TUNEL+ cells were determined for 5-6 different cultures (n = 5-6). Statistical analysis: One-way ANOVA with Tukey's multiple comparison test.

3.3.2.5. Fluorescent microscopy

Sections from either porcine eyes or organotypic retinal explant cultures were images using fluorescence microscopy (Axio Imager Z2 with ApoTome function, Zeiss, Oberkochen, Germany). A CCD camera and 10X or 20X objectives were used. For DiO signal: green channel of Ex./Em. of 483/501 nm. TUNEL assay: red channel of Ex./Em. 548/561 nm. DAPI signal: blue channel of Ex./Em. 353/465 nm. In all cases, the ApoTome function was used. Z-stacks were collected 1 µm across 25 images for porcine eye sections or 11 images for retinal explant cultures using the microscope software (ZEN 2.6, Zeiss). The images were projected using the Maximum Intensity Projection function, and these images were used for data analysis.

4. Results

4.1. Physico-chemical characterization of LNCs

Blank LNCs and loaded LNCs (drug or DiO loaded) were analyzed for particle size and size distribution (poly dispersity index; PDI) along with the zeta potential (Table 1). Particle size and zeta potential of unloaded and DiO loaded LNCs were similar, however an increased size and zeta potential was observed in the presence of encapsulated CN03 in agreement with earlier published data [7, 8]. Detailed physico-chemical characterization data on LNCs and liposomes ha been described in previous publications [7, 17].

Table 1. Characterization of LNCs. Data is represented as mean ± SD (n = 3)

Formulation	Particle size (diameter, nm)	PDI	Zeta potential (mV)
Blank LNCs	61 ± 1	0.03 ± 0.02	-2.5 ± 1.1
CN03-LNCs	72 ± 1	0.07 ± 0.02	-11.3 ± 0.8
DiO-LNCs	58 ± 0.2	0.04 ± 0.03	-0.3 ± 0.1

Further experiments were performed to quantify the release of DiO in phosphate buffer. Here, DiO release was insignificant and did not produce detectable levels of fluorescence even after

48 h of testing. This confirms that the dye is confined in the LNCs and can be used as a marker to study the distribution of LNC in the eye.

4.2. Tissue permeability studies

Permeability studies were performed with a Franz-diffusion cell system using excised tissues from intact porcine eyeballs. The permeability coefficients of free drug and the drug loaded particles across full-thickness cornea were 2.2 ± 1.2 x 10^{-8} cm/s, and 5.1 ± 1.7 x 10^{-8} cm/s respectively. For conjunctiva-sclera-choroid-retina the free drug and LNC/CN03 formulation showed a permeability coefficient of 1.0 ± 0.2 x 10^{-7} cm/s and 1.60 ± 0.4 x 10^{-7} cm/s respectively. Based on the permeability coefficients, the conjunctiva-sclera-choroid-retina was 4.6 times more permeable to the free compound than the full-thickness cornea and 3 times more permeable for the LNCs formulation. The cumulative drug penetration of drug and LNC/CN03 formulation in the excised ocular tissues are shown in **Fig. 2**.

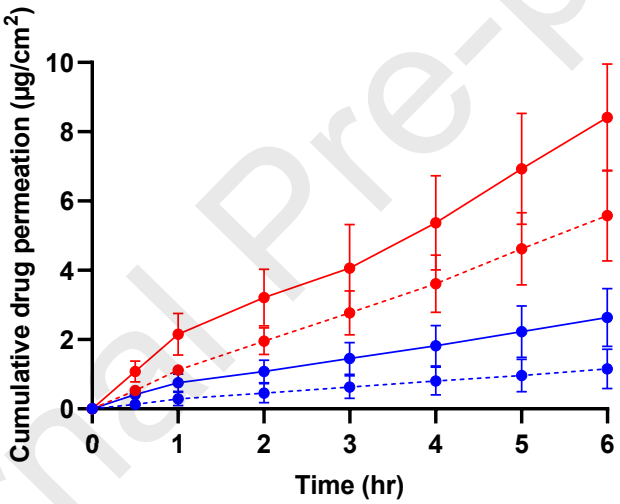

Fig. 2. Cumulative amount permeated per area (µg/cm^2, mean ± SD, n = 3) of CN03 (dashed lines) and LNC/CN03 formulation (solid lines). Data in Blue indicates the permeation through full-thickness cornea and the data in Red indicates the permeation through conjunctiva-sclera-choroid-retina.

4.3. Intraocular bio-distribution in *ex vivo* porcine eye

Fluorophotometry was used on intact *ex vivo* porcine eyes obtained from the local slaughterhouse to analyze the kinetics of the intravitreal diffusion of LNC. The fluorescent marker DiO was formulated with the LNCs to localize the particles within the axial length of the eyeball. Intensity plots as shown in **Fig. 3A** were collected across different time points up to 24 h post-injection. The area under the curve (AUC) for each time-point was plotted (**Fig. 3B**) to analyze how fast the LNCs were diffusing within the eye. After 24 h the AUC was

reduced to about 10 % the value of the peak, which occurred at 2 h post-injection. The initial increase in AUC from 0 to 2 h, may be due to a back-flow of the injected solution through the injection channel. The following decrease in signal is then caused by intravitreal diffusion.

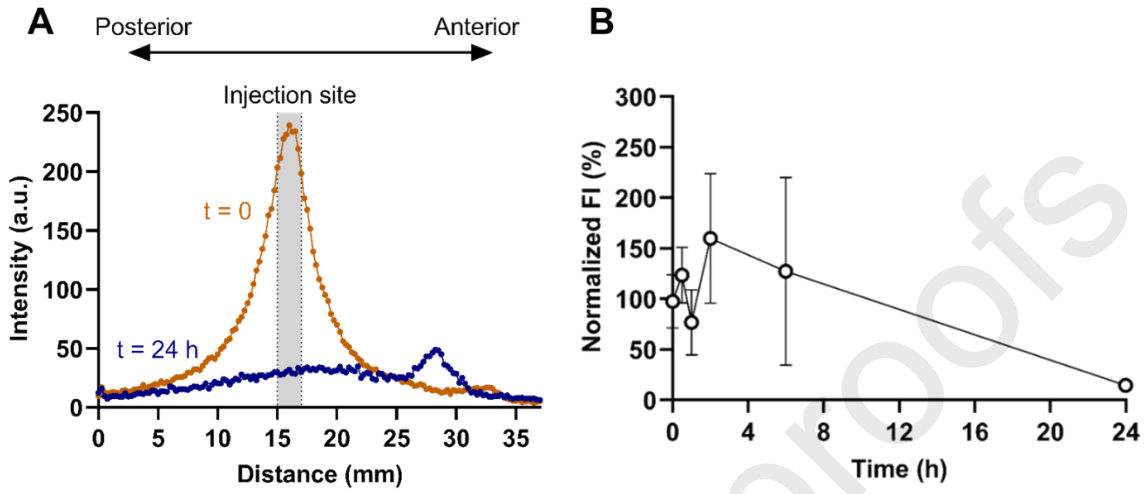

Fig. 3. Intravitreal movement of LNCs as determined by fluorophotometry. A Example profile of LNC-DiO signal from injected pig eyes at t = 0 (orange) and at t = 24 h (purple) along the axial length. B Normalized fluorescent intensity (FI) in the injection site from 0 to 24 h. Results present mean ± SD for n = 5 eyes.

4.4. Histological analysis of *ex vivo* porcine eyes

The fluorophotometry measurements revealed an almost even distribution of the injected LNC/DiO after 24 h (**Fig. 3**). Fluorescence microscopy was then used to record the DiO signal from different regions of the eye (**Fig. 4A**). For comparison, conventional POPC-liposomes with 5 mol% 2 kDa mPEG were also tested. The DiO signal was measured from the images using the same microscopy conditions across all specimens (**Fig. 4B**). No statistically significant differences were observed between LNCs and liposomes except at the ciliary body where more LNCs than liposomes accumulated. Liposomes tended to absorb more strongly to the retina, although this was not statistically significant. Qualitatively, it was observed that LNCs were primarily restricted to the surface of the retina around the vitreoretinal interface, while the liposomal DiO was transported through the whole retina (see **Fig. 4A**, panels labelled "retina"). Also, the liposomal distribution in the vitreous seemed to be more homogenous compared to the LNCs. An overview of the intraocular bio-distribution is shown in **Fig. 4C**.

Journal Pre-proofs

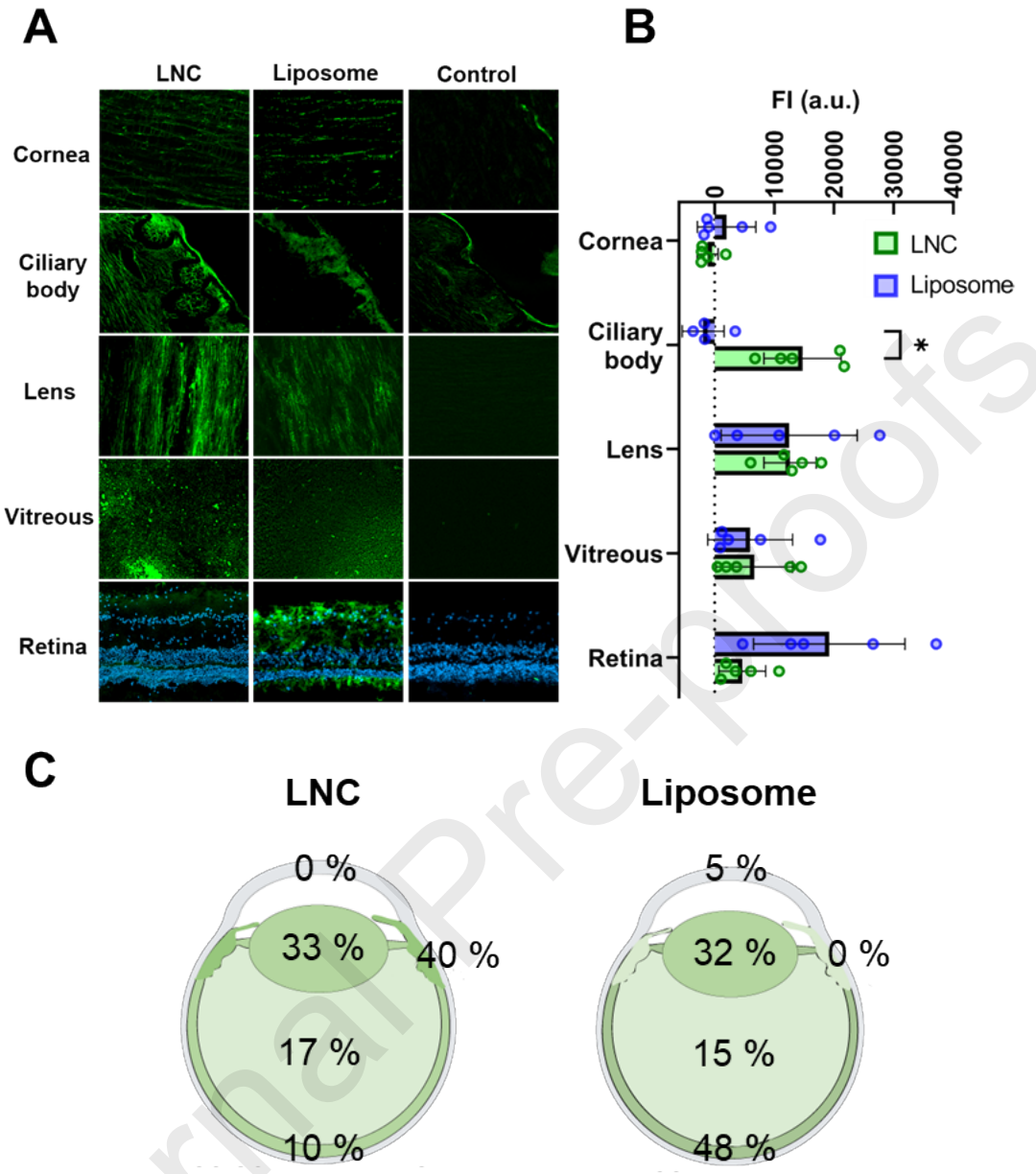

Fig. 4. Bio-distribution of LNCs and liposomes after intravitreal administration in whole porcine eyes. (A) Microscopy images of different tissues from sections of porcine eyes 24 h after injection of either LNC/DiO formulation or liposome/DiO formulation or non-injected eyes (control). Scale bar = 50 µm. (B) Fluorescent intensities (FI) from relevant ocular tissues after injection of LNCs or liposomes. Negative value is due to subtraction of background signal. Results represent mean ± SD for n = 5, * $p \leq 0.05$. Data analysis: Two-way ANOVA with Šidák's multiple comparison test. (C) Schematic drawings illustrating the relative distribution of LNCs and liposomes in pig eyes.

4.5. Retinal toxicity profile

Retinal explants derived from P9 mice and cultured for four days were used to assess the toxicity of LNCs to the retina. Without LNC addition to the cultures, there were around 2 % TUNEL-positive cells in the ONL, reflecting the cell death rate caused by the explant situation

Journal Pre-proofs

itself. Cell death in the INL was very low, indicating that INL cells were less sensitive than photoreceptors. At a concentration of 1 mg/mL LNCs appeared to be well tolerated by the retina. However, at 5 mg/mL there was a tendency towards increased cell death. At an LNC concentration of 10 mg/mL, a statistically significant increase in the number of dying cells in the ONL was observed, suggesting that this concentration was toxic to photoreceptors (**Fig. 5**). In all cases, there was no change in the cell death in the INL.

It is important to consider that the LNC concentration was tested on the retina itself. Since an injected formulation would be diluted in the vitreous, the concentration of the highest tolerated dose could be a lot higher than 1 mg/mL. The human vitreous is about 4-5 mL [27], and if 50 µL of the LNC formulation was injected, a dose of 80 mg/mL could be given to achieve a local concentration at the retina of 1 mg/mL. However, this is assuming an even distribution in the eye, which our bio-distribution results do not support (**Fig. 4**), so that the local concentration at the retina would likely be lower than expected.

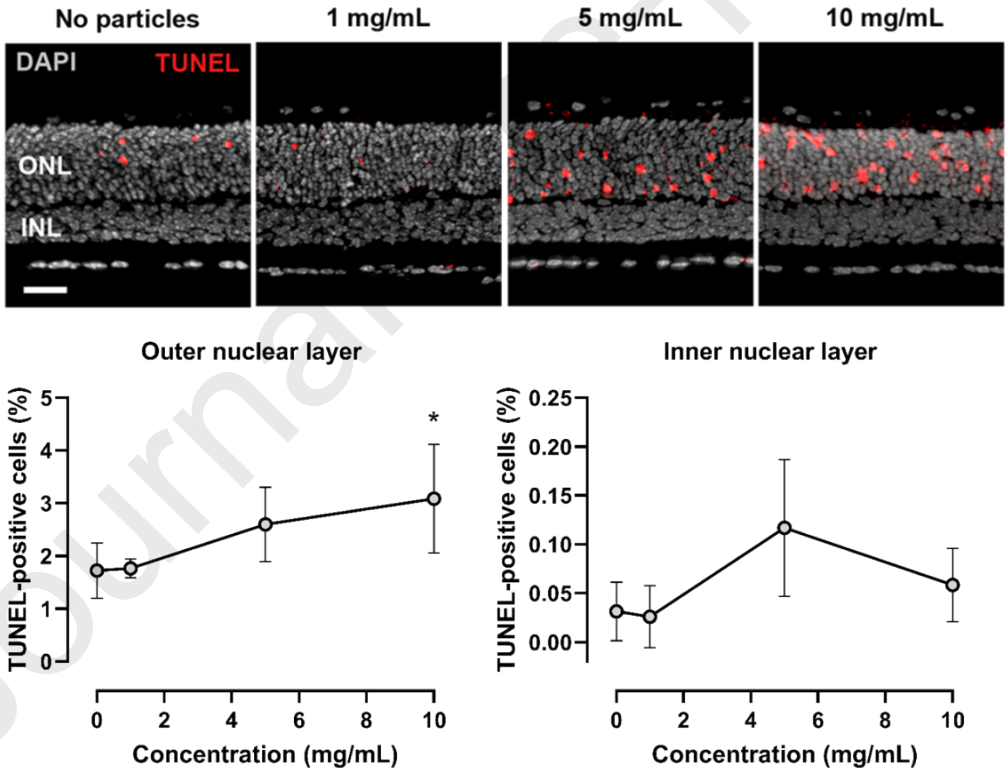

Fig. 5. Retinal toxicity profile of LNCs. Retinal explant cultures derived from WT mice were incubated with LNCs at different concentrations for 4 days. The TUNEL-assay (red) was employed to label dying cells in tissue sections. DAPI (gray) was used as nuclear counterstain to visualize the outer nuclear layer (ONL) and inner nuclear layer in the retina (INL). The number of TUNEL-positive cells in either layer was analyzed. Notice the differences in scales between the two graphs, indicating that cell death related mostly to photoreceptors in the ONL.

Scale bar = 50 µm. Results represent mean ± SD for n = 4-5 animals. * $p \leq 0.05$. Statistical analysis: One-way ANOVA with Tukey's post-hoc test.

4.6. Treatment efficacy of encapsulated drugs

Retinas from the retinal degeneration mouse model, *rd1*, were used to assess the treatment efficacy of CN03 encapsulated in LNC. Since the LNCs were tested for an intravitreal administration route, all drug solution was applied on top of the cultures (*i.e.*, from the ganglion cell side). In an *in vivo* setting, using intravitreal injection, the LNCs would reach the retina from this side. Either a free drug solution (free CN03), LNC/CN03 formulation, or non-treated control retinas were analyzed. For drug-containing solutions, the concentration in the solution administered was 200 µM. Assuming equal distribution in the tissue and culture medium, the final drug concentration was 4 µM. Explant cultures derived from wild-type mice were compared. As in the toxicity analysis, a TUNEL-assay was used to detect dying photoreceptors in cross-sections of the tissue (**Fig. 6**).

In *rd1* retinas, there was a significant increase in dying photoreceptors compared to wild-type. Both the free drug and the LNC encapsulated drug provided a protection of the photoreceptors as evidenced by a lower TUNEL-positive cell count. In both cases, cell death was reduced by 25 %. The release of CN03 from LNC/CN03 formulation was fast enough to have an effect on the *rd1* model, and this effect was found to be similar to that of free CN03. Although there was no difference between the CN03 and LNC/CN03 formulation treatments in this *in vitro* setting, in the *in vivo* situation LNCs could be advantageous to retain the drug within the vitreous and thereby improve the pharmacokinetics of CN03 and extend its pharmacological effect.

Journal Pre-proofs

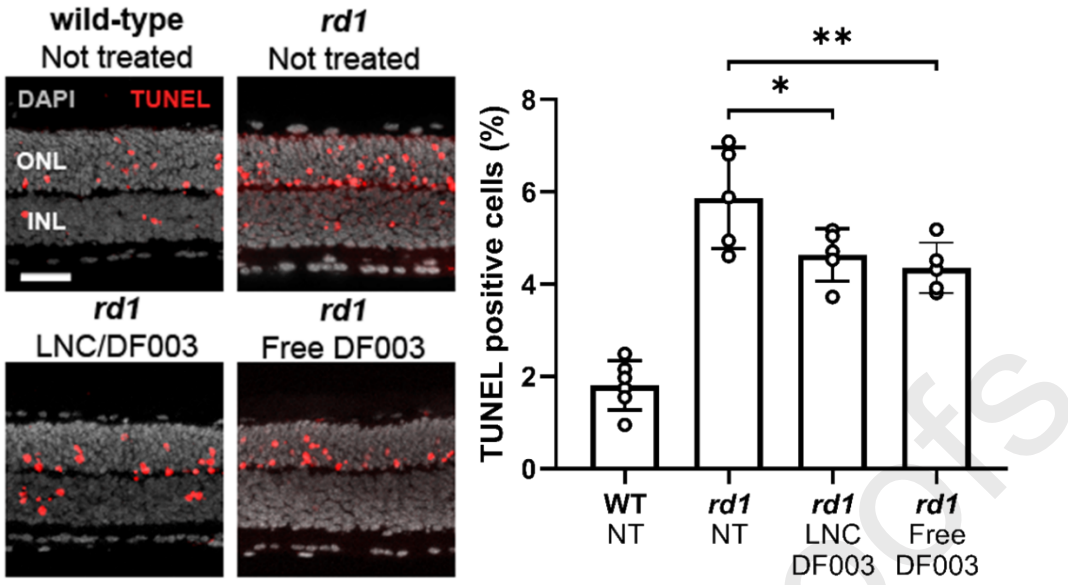

Fig. 6. Treatment efficacy of the LNC/drug formulation. Retinal explant cultures derived from the *rd1* mouse model were treated with the retinoprotective drug CN03, either in a particle-free solution (Free CN03) or LNC/CN03 formulation. In both cases, drug concentration in the treatment solutions was 200 µM, and all were applied on top of the retinal culture. Assuming equal distribution in the culture medium, the final concentration was 4 µM. Treatment period was from P7 to P11. A TUNEL-assay (red) was used to detect dying cells in cross-sections of the cultures, and DAPI (gray) was used to localize the outer nuclear layer (ONL) and inner nuclear layer (INL). The amount of dying cells (TUNEL-positive cells) in the ONL was counted to assess treatment effects. Scale bar = 50 µm. Results represent mean ± SD for n = 5-6 animals. * $p \leq 0.05$, ** $p \leq 0.01$ compared to the *rd1* not treated (NT) condition. Statistical analysis: One-way ANOVA with Tukey's post-hoc test.

5. Discussion

In this study, we employed different *ex vivo* and *in vitro* techniques to determine the effectiveness of LNCs as an intraocular delivery system for the neuroprotective drug CN03. The data address several aspects that are useful for the development of ocular drug delivery systems, such as particle size, vitreal mobility, ocular tissue accumulation, retinal toxicity, and treatment efficacy in retinal cultures.

Characterization of LNCs indicated that the formulation, irrespective of presence or absence of a loaded cargo, resulted in particles with < 100 nm in size and with a narrow particle size distribution. An increase in size as measured with DLS was observed when the drug CN03 was loaded in the particles. In such particles, the surface charge, as measured by the zeta potential, became more negative compared to unloaded LNCs, indicating that CN03 was present on the surface of the particles. These observations are in accordance with previous findings [7, 8]. On the other hand, DiO loading did not seem to impact either particle size or zeta potential.

Lipophilic DiO is expected to predominantly locate to the core of the particles, causing little change to the surface charge. To study the integrity of DiO loaded particles and confirm the suitability of DiO as a fluorescent label for LNCs, release experiments were performed in phosphate buffer. No DiO release to the medium could be detected for up to 48 h. Apparently, a strong interaction of DiO with the oily core, as well as poor solubility of DiO in phosphate buffer prevented the label release from the LNC.

The cornea of the eye forms a tremendous barrier for the penetration of drug substances. To reach therapeutic drug concentrations in the retina, topical administration is usually not sufficient and intravitreal injection may be required to achieve the desired effect [28, 29]. It has however been reported that lipid-based nanoparticles enhance the ocular penetration of drugs which are targeted for both anterior and posterior chambers when administered topically to the eye [30-35]. Thus, to study the ability of the LNCs in improving the ocular penetration, permeability screening of free CN03 and CN03 loaded LNCs was conducted on both full-thickness cornea and conjunctiva-sclera-choroid-retina excised from fresh porcine eyeballs using Franz-diffusion cells methodology [22, 23].

The permeability of CN03 was found to be improved across both full-thickness cornea and conjunctiva-sclera-choroid-retina when formulated with LNCs compared to CN03 alone in solution. Moreover, the permeability coefficients of both drug solution and the CN03-LNCs across conjunctiva-sclera-choroid-retina were higher than across full-thickness cornea. However, the LNC permeability values were relatively low in comparison to other ophthalmologic drugs, the *ex vivo* permeability of which has been tested by other authors using a similar methodology (Table 2). In a study performed by Lorenzo-Soler *et al*. (manuscript under revision), where 27 different drugs were tested in their free form using the methodology here described, the mean permeability coefficients across both tissues were calculated. The mean permeability values of the compounds tested were $5.0 \pm 0.3 \times 10^{-6}$ cm/s across full thickness cornea and $16.0 \pm 0.9 \times 10^{-6}$ cm/s for conjunctiva-sclera-choroid-retina. These values are considerably higher than those shown for CN03, indicating a poor permeability of the compound across both cornea and the scleral complex. This suggests that the topical route of administration is not an efficient route for delivering CN03 to the retinal photoreceptors.

Table 2. Permeability of drug compounds across ocular tissues derived from porcine eyeballs.

Compound	Application	Tissue permeability (cm/s)		Reference(s)
		Full-thickness cornea	Conjunctiva-sclera-choroid-retina	
Dexamethasone	Glucocorticoid used in treatment of allergic reactions in the eye	$0.2 \pm 0.1 \times 10^{-6}$ - $7.6 \pm 1.2 \times 10^{-6}$	$1.0 \pm 0.2 \times 10^{-6}$	[36-39]
Propranolol	Beta-blockers used in the treatment of intraocular pressure	$1.5 \pm 1.4 \times 10^{-6}$ - $14.6 \pm 0.5 \times 10^{-6}$	$7.0 \pm 2.5 \times 10^{-6}$	[22, 23, 37]
Timolol maleate		$5.1 \pm 0.6 \times 10^{-6}$ - $10.7 \pm 2.1 \times 10^{-6}$	$1.3 \pm 0.4 \times 10^{-6}$	[36, 38, 39]
Library of compounds with varied molecular properties (n = 27)	Varied applications	$5.0 \pm 0.3 \times 10^{-6}$	$16.0 \pm 0.9 \times 10^{-6}$	Unpublished *

* Data reported as mean permeability values from 27 different compounds

For histology and ocular distribution experiments, we used fresh porcine eyes from the slaughterhouse. The excised porcine eyes have several advantages over *in vivo* studies such as cost, ethical concerns of animal use, and rapid production of data [40]. Moreover, porcine eyes from slaughterhouses are readily available in many parts of the world. However, it is also important to consider the limitations of using this model. Due to the degradation of the eyes following the tissue isolation, longer term studies are usually not possible. We have previously demonstrated that porcine eyes are useful in short term pharmacokinetic analyses in combination with fluorophotometry [17], but even under sterile conditions, obvious signs of tissue degradation can be seen after 5-7 days. In this study, we have used the porcine eyes within approximately 4 h following their excision, *i.e.* long before tissue degradation sets in. Our porcine eye data showed considerable variability with standard deviations in eye distribution of up to 100 % for 5 experiments. This may be due to experimental differences in individual intravitreal injections, as well as differences in the porcine eyes themselves. Other studies that used intact *ex vivo* porcine eyes also reported high variation [18].

Fluorophotometry measurements on intact porcine eyes showed a near complete distribution of DiO-LNCs 24 h post injection, showing that the distribution of particles is unhindered by the vitreous network. From the histological analysis of injected porcine eyes, both liposomes and LNCs showed similar total fluorescence intensities 24 h after injection, yet their distribution to different ocular tissues was markedly different. LNCs tended to accumulate on the surface of the ciliary body more than liposomes. Uptake of liposomes in the ciliary

Journal Pre-proofs

epithelium may be limited by the PEG layer on the surface of the liposomes [41]. For the retina, on the other hand, the PEG layer may stimulate uptake as shown in the work of Tavakoli *et al*. [42]. They showed that PEGylation of liposomes improves the permeation across the inner limiting membrane of the retina, thereby increasing the possibilities for retinal cell uptake. Still, it should be noted that, since hydrophobic molecules were used as tracers, transfer of the tracer from the lipid bilayer to hydrophobic biological membranes in the retina is possible. This may happen more often for lipids with low transition temperatures like POPC used in this study [43]. Since DiO is encapsulated in the inner core in the LNC, it is likely that the transfer happens less than for the liposomes. Further, for both LNCs and liposomes, fluorescence signal was evident across the lens, which may be due to the lipophilic nature of DiO [44].

We found that LNCs were largely non-toxic to the retina with only a slight increase in the number of dying photoreceptors after *in vitro* exposure to concentrations of 10 mg/mL. Low cytotoxicity at the studied LNC concentration may in part be due to the poor retinal uptake of the LNCs. In comparison, liposomes, which showed higher retinal penetration, were found to be slightly toxic at 5 mg/mL [17]. Other studies have also found higher retinal penetration of liposomes [17, 45, 46], as well as other nano-systems like albumin-based nanoparticles [47, 48] and PLGA-based nanoparticles [49] compared to LNCs. The poor retinal uptake of LNCs likely affects drug transport, which, in retinal cultures, was not improved by the LNCs. Yet, in the treatment of retinal explant cultures, the encapsulated drug provided the same level of protection as the free drug solution. Thus, the LNCs may not need to be taken up by the retina to allow the loaded drug to exert its effect. The main benefit of the LNCs as an intraocular drug delivery system may therefore be their ability to provide a drug depot and sustain the release of CN03 in the vitreous over a prolonged period of time [7]. Moreover, a poor retinal uptake of LNCs could prolong their half-life in the eye as retinal uptake is a route of elimination from the vitreous [50]. Both factors would reduce the required number of IVT injections, something highly advantageous in a clinical context.

6. Conclusion

In summary, LNCs were well suited for encapsulation of the small molecule drug CN03 and exhibited low retinal toxicity. The bio-distribution of LNCs in the vitreous of *ex vivo* porcine eyes revealed a high degree of permeation in the ciliary body compared to the retina, indicating that LNCs might be useful for targeted delivery to the ciliary body. Nevertheless, in explanted *in vitro* retinal cultures LNC formulated CN03 could efficiently protect *rd1* mouse photoreceptors from mutation-induced degeneration.

Journal Pre-proofs

Acknowledgements

The authors would like to thank Professor Thorsteinn Loftsson at the University of Iceland for his continued support and guidance, particularly to Dileep Urimi as an academic supervisor. The authors would like to thank Ronja Widenbring for her review and proof reading of this manuscript.

Funding sources

This work was financially supported by the German Research Council (DFG; PA1751/10-1), and the European Union (*trans*Med, H2020-MSCA-ITN-2017-765441), European Joint Programme on Rare Diseases - Joint Transnational Call 2020 (TreatRP).

Declaration of Competing Interest

The authors declare that they have no known competing financial interests or personal relationships that could have appeared to influence the work reported in this paper.

Journal Pre-proofs

References

1. Sahaboglu, A., et al., *Retinitis pigmentosa: rapid neurodegeneration is governed by slow cell death mechanisms.* Cell Death Dis, 2013. **4**(2): p. e488.
2. Paquet-Durand, F., et al., *PKG activity causes photoreceptor cell death in two retinitis pigmentosa models.* Journal of Neurochemistry, 2009. **108**(3): p. 796-810.
3. Sancho-Pelluz, J., et al., *Photoreceptor cell death mechanisms in inherited retinal degeneration.* Mol Neurobiol, 2008. **38**(3): p. 253-69.
4. Liu, L. and X. Liu, *Roles of Drug Transporters in Blood-Retinal Barrier*, in *Drug Transporters in Drug Disposition, Effects and Toxicity*, X. Liu and G. Pan, Editors. 2019, Springer Singapore: Singapore. p. 467-504.
5. Farber, D.B. and R.N. Lolley, *Cyclic guanosine monophosphate: elevation in degenerating photoreceptor cells of the C3H mouse retina.* Science, 1974. **186**(4162): p. 449-51.
6. Vighi, E., et al., *Combination of cGMP analogue and drug delivery system provides functional protection in hereditary retinal degeneration.* Proceedings of the National Academy of Sciences, 2018. **115**(13): p. E2997-E3006.
7. Urimi, D., et al., *Formulation development and upscaling of lipid nanocapsules as a drug delivery system for a novel cyclic GMP analogue intended for retinal drug delivery.* Int J Pharm, 2021. **602**: p. 120640.
8. Urimi, D., et al., *Structural Characterization Study of a Lipid Nanocapsule Formulation Intended for Drug Delivery Applications Using Small-Angle Scattering Techniques.* Molecular pharmaceutics, 2022. **19**(4): p. 1068-1077.
9. Panwar, P., et al., *Preparation, characterization, and in vitro release study of albendazole-encapsulated nanosize liposomes.* Int J Nanomedicine, 2010. **5**: p. 101-8.
10. Miao, Z.L., et al., *Preparation of a liposomal delivery system and its in vitro release of rapamycin.* Exp Ther Med, 2015. **9**(3): p. 941-946.
11. Sun, R., et al., *Ultra-small-size Astragaloside-IV loaded lipid nanocapsules eye drops for the effective management of dry age-related macular degeneration.* Expert Opinion on Drug Delivery, 2020. **17**(9): p. 1305-1320.
12. Formica, M.L., et al., *Novel hybrid lipid nanocapsules loaded with a therapeutic monoclonal antibody–Bevacizumab–and Triamcinolone acetonide for combined therapy in neovascular ocular pathologies.* Materials Science and Engineering: C, 2021. **119**: p. 111398.
13. Formica, M.L., et al., *Triamcinolone acetonide-loaded lipid nanocapsules for ophthalmic applications.* International Journal of Pharmaceutics, 2020. **573**: p. 118795.
14. Maurice, D.M., *Drug delivery to the posterior segment from drops.* Surv Ophthalmol, 2002. **47 Suppl 1**: p. S41-52.
15. Bochot, A. and E. Fattal, *Liposomes for intravitreal drug delivery: A state of the art.* Journal of Controlled Release, 2012. **161**(2): p. 628-634.
16. García-Quintanilla, L., et al., *Pharmacokinetics of Intravitreal Anti-VEGF Drugs in Age-Related Macular Degeneration.* Pharmaceutics, 2019. **11**(8).
17. Christensen, G., et al., *Investigating Ex Vivo Animal Models to Test the Performance of Intravitreal Liposomal Drug Delivery Systems.* Pharmaceutics, 2021. **13**(7).
18. Eriksen, A.Z., et al., *The diffusion dynamics of PEGylated liposomes in the intact vitreous of the ex vivo porcine eye: A fluorescence correlation spectroscopy and biodistribution study.* Int J Pharm, 2017. **522**(1-2): p. 90-97.
19. Pérez, O., N. Schipper, and M. Bollmark, *Preparative Synthesis of an R P-Guanosine-3', 5'-Cyclic Phosphorothioate Analogue, a Drug Candidate for the Treatment of Retinal Degenerations.* Organic process research & development, 2021. **25**(11): p. 2453-2460.
20. Zhang, H., *Thin-Film Hydration Followed by Extrusion Method for Liposome Preparation*, in *Liposomes: Methods and Protocols*, G.G.M. D'Souza, Editor. 2017, Springer New York: New York, NY. p. 17-22.

Journal Pre-proofs

21. Nicoli, S., et al., *Porcine sclera as a model of human sclera for in vitro transport experiments: histology, SEM, and comparative permeability.* Molecular vision, 2009. **15**: p. 259.
22. Pescina, S., et al., *Development of a convenient ex vivo model for the study of the transcorneal permeation of drugs: histological and permeability evaluation.* Journal of pharmaceutical sciences, 2015. **104**(1): p. 63-71.
23. Pescina, S., et al., *Ex vivo models to evaluate the role of ocular melanin in trans-scleral drug delivery.* European journal of pharmaceutical sciences, 2012. **46**(5): p. 475-483.
24. Niedorf, F., E. Schmidt, and M. Kietzmann, *The automated, accurate and reproducible determination of steady-state permeation parameters from percutaneous permeation data.* Alternatives to Laboratory Animals, 2008. **36**(2): p. 201-213.
25. Belhadj, S., et al., *Long-Term, Serum-Free Cultivation of Organotypic Mouse Retina Explants with Intact Retinal Pigment Epithelium.* Journal of Visualized Experiments, 2020.
26. Loo, D.T., *In situ detection of apoptosis by the TUNEL assay: an overview of techniques.* Methods in molecular biology, 2011. **682**: p. 3-13.
27. Azhdam, A.M., R.A. Goldberg, and S. Ugradar, *In Vivo Measurement of the Human Vitreous Chamber Volume Using Computed Tomography Imaging of 100 Eyes.* Transl Vis Sci Technol, 2020. **9**(1): p. 2.
28. Agrahari, V., et al., *How are we improving the delivery to back of the eye? Advances and challenges of novel therapeutic approaches.* Expert opinion on drug delivery, 2017. **14**(10): p. 1145-1162.
29. Kaur, I.P. and S. Kakkar, *Nanotherapy for posterior eye diseases.* Journal of Controlled Release, 2014. **193**: p. 100-112.
30. Davis, B.M., et al., *Topical delivery of Avastin to the posterior segment of the eye in vivo using annexin A5-associated liposomes.* Small, 2014. **10**(8): p. 1575-1584.
31. Gaballa, S.A., et al., *Preparation and evaluation of cubosomes/cubosomal gels for ocular delivery of beclomethasone dipropionate for management of uveitis.* Pharmaceutical Research, 2020. **37**(10): p. 1-23.
32. Khalil, R.M., et al., *Enhancement of lomefloxacin Hcl ocular efficacy via niosomal encapsulation: in vitro characterization and in vivo evaluation.* Journal of liposome research, 2017. **27**(4): p. 312-323.
33. Lakhani, P., et al., *Optimization, stabilization, and characterization of amphotericin B loaded nanostructured lipid carriers for ocular drug delivery.* International journal of pharmaceutics, 2019. **572**: p. 118771.
34. Navarro-Partida, J., et al., *Safety and tolerability of topical ophthalmic triamcinolone acetonide-loaded liposomes formulation and evaluation of its biologic activity in patients with diabetic macular edema.* Pharmaceutics, 2021. **13**(3): p. 322.
35. Tatke, A., et al., *In situ gel of triamcinolone acetonide-loaded solid lipid nanoparticles for improved topical ocular delivery: Tear kinetics and ocular disposition studies.* Nanomaterials, 2018. **9**(1): p. 33.
36. Juretić, M., et al., *Biopharmaceutical evaluation of surface active ophthalmic excipients using in vitro and ex vivo corneal models.* European Journal of Pharmaceutical Sciences, 2018. **120**: p. 133-141.
37. Ramsay, E., et al., *Corneal and conjunctival drug permeability: Systematic comparison and pharmacokinetic impact in the eye.* European Journal of Pharmaceutical Sciences, 2018. **119**: p. 83-89.
38. Loch, C., et al., *Determination of permeability coefficients of ophthalmic drugs through different layers of porcine, rabbit and bovine eyes.* European journal of pharmaceutical sciences, 2012. **47**(1): p. 131-138.
39. Hahne, M., et al., *Prevalidation of a human cornea construct as an alternative to animal corneas for in vitro drug absorption studies.* Journal of pharmaceutical sciences, 2012. **101**(8): p. 2976-2988.

Journal Pre-proofs

40. Heikkinen, E.M., et al., *Esterase activity in porcine and albino rabbit ocular tissues.* European Journal of Pharmaceutical Sciences, 2018. **123**: p. 106-110.
41. Hatakeyama, H., H. Akita, and H. Harashima, *The polyethyleneglycol dilemma: advantage and disadvantage of PEGylation of liposomes for systemic genes and nucleic acids delivery to tumors.* Biol Pharm Bull, 2013. **36**(6): p. 892-9.
42. Tavakoli, S., et al., *Ocular barriers to retinal delivery of intravitreal liposomes: Impact of vitreoretinal interface.* Journal of Controlled Release, 2020. **328**: p. 952-961.
43. Urquhart, A.J. and A.Z. Eriksen, *Recent developments in liposomal drug delivery systems for the treatment of retinal diseases.* Drug Discov Today, 2019. **24**(8): p. 1660-1668.
44. Heikkinen, E.M., et al., *Distribution of small molecular weight drugs into the porcine lens: studies on imaging mass spectrometry, partition coefficients, and implications in ocular pharmacokinetics.* Molecular pharmaceutics, 2019. **16**(9): p. 3968-3976.
45. Lee, J., et al., *Effective Retinal Penetration of Lipophilic and Lipid-Conjugated Hydrophilic Agents Delivered by Engineered Liposomes.* Molecular Pharmaceutics, 2017. **14**(2): p. 423-430.
46. Camelo, S., et al., *Ocular and systemic bio-distribution of rhodamine-conjugated liposomes loaded with VIP injected into the vitreous of Lewis rats.* Molecular Vision, 2007. **13**.
47. Kim, H., S.B. Robinson, and K.G. Csaky, *Investigating the Movement of Intravitreal Human Serum Albumin Nanoparticles in the Vitreous and Retina.* Pharmaceutical Research, 2009. **26**(2).
48. Koo, H., et al., *The movement of self-assembled amphiphilic polymeric nanoparticles in the vitreous and retina after intravitreal injection.* Biomaterials, 2012. **33**(12): p. 3485-93.
49. Bourges, J.L., et al., *Ocular drug delivery targeting the retina and retinal pigment epithelium using polylactide nanoparticles.* Invest Ophthalmol Vis Sci, 2003. **44**(8): p. 3562-9.
50. Amo, E.M.d., et al., *Pharmacokinetic aspects of retinal drug delivery.* Progress in Retinal and Eye Research, 2017. **57**: p. 134-185.

Journal Pre-proofs

Graphical Abstract

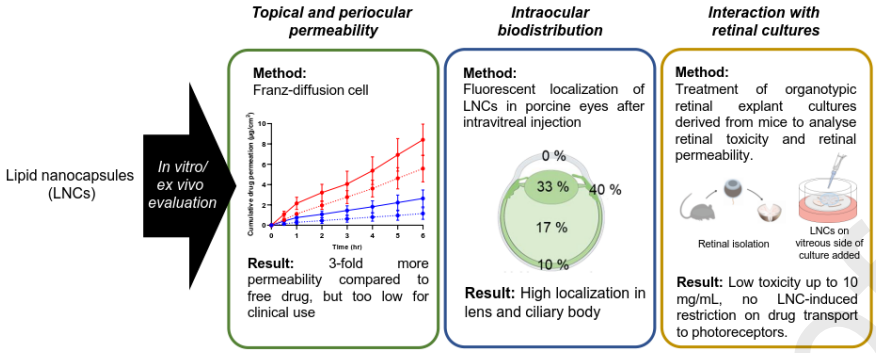

Journal Pre-proofs